

# Dislocation Density Reduction in GaSb Films Grown on GaAs Substrates by Molecular Beam Epitaxy

W. Qian\* and M. Skowronski

Department of Materials Science and Engineering, Carnegie Mellon University, Pittsburgh, Pennsylvania 15213, USA

R. Kaspi

Wright-Patterson Air Force Base, Wright Laboratory, Avionics Directorate, Ohio 45433, USA

## ABSTRACT

The reduction of threading dislocation density due to their mutual interactions in GaSb thin films grown on (001) GaAs substrates by molecular beam epitaxy has been investigated. The effectiveness of several buffer layer schemes including GaSb/AlSb strained layer superlattice and  $\text{In}_{0.11}\text{Ga}_{0.89}\text{Sb}/\text{GaAs}$  buffers for threading dislocation suppression was evaluated. High-resolution transmission electron microscopy shows that the GaSb/GaAs interface consists of a highly periodic network of  $90^\circ$  pure edge misfit dislocations, with an average spacing close to that for a fully relaxed system. This results in relatively low threading densities in the GaSb epilayer, despite their large lattice constant mismatch (8.2%). The threading dislocation density as a function of GaSb film thickness was determined by plan-view transmission electron microscopy and was found to decrease with film thickness due to mutual interactions among dislocations. It was found that a strained layer superlattice of GaSb/AlSb, with each layer close to its critical thickness, is the most effective in threading density reduction.

## Introduction

The GaSb/GaAs heterostructure has been of increased interest in recent years because of its potential applications in optoelectronic devices. For instance, thin GaSb films grown on GaAs can be used as convenient composite substrates for InAs/InGaSb type II strained layer superlattice infrared detectors. The high concentration of native acceptors and the associated free holes presented in bulk GaSb crystals make the GaSb wafers opaque in the infrared and eliminate the most convenient detector design with illumination from the back side. A thin film of relaxed GaSb deposited on GaAs would be a good alternative to bulk GaSb substrates. However, high density of defects (mainly threading dislocations) originating from the GaSb/GaAs interface and propagating through the entire structure affect both the electrical and optical properties of the superlattice, thus limiting detector performance. Also, the dislocation cores are known to form non-radiative recombination centers which limit the efficiency of light emitting diodes and often lead to injection failures in lasers.<sup>1</sup> Therefore, it is of practical importance to minimize the threading dislocation density in the GaSb thin films during epitaxial growth.

The misfit dislocations along the lattice-mismatched heterointerface are a thermodynamic necessity, (for thick films) but the threading dislocations could, in principle, be entirely avoided. However, due to kinetic limitations of the strain relaxation process, threading dislocations are almost always present in films at thicknesses which are of practical use for device applications. Considerable effort has been expended on reduction of threading dislocation densities in heteroepitaxial III-V semiconductors, such as, for example, GaAs grown on Si.<sup>1,2</sup> Techniques which have been proved to be partially effective for threading dislocation reduction in the GaAs/Si system include strained layer superlattices,<sup>3-5</sup> step- and continuously graded buffer layers,<sup>6</sup> and postgrowth annealing.<sup>1,7</sup> By comparison, relatively little is known about the threading dislocations in epitaxial films grown on substrates with very large lattice mismatches, such as (001) GaSb/GaAs which has a 8.2% lattice constant and 16% thermal expansion coefficient mismatches. A recent study on the GaSb/GaAs heteroepitaxial system revealed some interesting features associated with its misfit strain relaxation.<sup>8-10</sup> Both the GaAs and GaSb are polar semiconductors having the cubic zinc blende structure, with space group  $F\bar{4}3m$ . However, it was

found that the strain due to its lattice mismatch has been well accommodated by a regular net of  $90^\circ$  pure edge misfit dislocations, and the GaSb epi layer can be characterized as strain-free.<sup>9</sup> This was attributed to a special GaAs surface treatment (the growth of an initial GaAs buffer layer) before the GaSb epitaxial growth.<sup>8</sup> Our investigation of the initial stages of molecular beam epitaxy (MBE) of GaSb on (001) GaAs demonstrated that up to nominal thickness of 50 Å, GaSb forms isolated coherent islands with highly periodic nets of  $90^\circ$  misfit dislocations at the interface which nucleate homogeneously at the leading edges of advancing {111} planes.<sup>10</sup> The primary source of threading dislocations in the GaSb film are the minority  $60^\circ$  misfit dislocations. These can either nucleate at the growth surface of the film and glide into the interface along the {111} slip planes or be introduced during island coalescence at later stages of growth.

This paper reports investigation of threading dislocation density reduction in GaSb thin films grown on (001) GaAs substrates. The film thickness dependence of threading dislocation densities has been determined from the measurements carried out in plan-view transmission electron microscopy (TEM) over a series of samples with different GaSb thicknesses. The effectiveness of several buffer layer schemes on threading dislocation reduction and the use of superlattice (SLS) for threading dislocation suppression have been investigated. The mechanism for threading dislocation reduction, either through their mutual interaction or by use of external strains, has been discussed in the light of our observations.

## Experimental

GaSb thin films were grown on (001) GaAs substrates by MBE. After thermal desorption of oxide at  $590^\circ\text{C}$  under an  $\text{As}_2$  overpressure, a 200 Å GaAs layer was deposited to provide a clean starting surface. Prior to the deposition of GaSb layers, the GaAs surface was held under an  $\text{Sb}_2$  flux for 60 s while the  $\text{As}_2$  cracker valve was closed and the substrate temperature was lowered. During this time, the arsenic background partial pressure dropped below  $3 \times 10^{-9}$  Torr. All GaSb layers were deposited at  $550^\circ\text{C}$  with an antimony stabilized surface exhibiting a  $1 \times 3$  reconstruction. The growth rate was approximately 0.8 monolayer per second. Following the growth of the GaSb layers, the wafer was cooled to  $300^\circ\text{C}$  under a  $\text{Sb}_2$  flux, at which point the antimony shutter was closed and the wafer was cooled down to room temperature. The base pressure of the MBE system was in the low  $10^{-10}$  Torr range. Typical heterostructure and electron optical properties of the selected

\* Present address: Department of Materials Science and Engineering, Northwestern University, Evanston, Illinois 60208, USA.

Table I. Heterostructure and electrical properties of the GaSb films.

Sample numbers	Buffer layer	Buffer thickness (Å)	Overlayer	Overlayer thickness (μm)	Resistivity (Ω-cm) (77 K)	$n(\text{cm}^{-3})$ (77 K)	Mobility ( $\text{cm}^2/\text{V s}$ ) (77 K)	PL peak energy (nm)	Absorption bandedge (nm)
601	GaSb	170	GaSb	1.2	0.2	$1.3\text{E}16$	2408	1614	1530
605	AlSb	1000	GaSb	1.2	0.23	$9.7\text{E}15$	2833	1638	1532
719	None		GaSb	0.5	0.15-RT	$8.1\text{E}16$	497-RT		
721	InGaSb	1000	GaSb	1.1	0.14-RT	$7.7\text{E}16$	565-RT	1638	
722	AlSb	5000	GaSb	1.1	0.25-RT	$3.5\text{E}16$	698-RT	1625	
723	AlSb	2000	GaSb	1.1	0.33-RT	$3.8\text{E}16$	506-RT	1631	
724	AlSb/GaSb	$(1000/1000) \times 4.5$	GaSb		0.11	$1.9\text{E}16$	3158		
				1.1	0.15-RT	$6.6\text{E}16$	635	1617	1539
725	None		GaSb		0.16	$1.1\text{E}16$	3615		
				5	0.25-RT	$3.7\text{E}16$	694-RT		1535

GaSb samples are listed in Table I. In order to study the film thickness dependence of threading dislocation densities, a set of samples was grown at nominally identical conditions with GaSb film thicknesses varying from 0.5 to 14 μm. Another set of samples with different buffer layer structures (AlSb or  $\text{In}_{0.11}\text{Ga}_{0.89}\text{Sb}$ ) was grown in order to study the effectiveness of SLS for threading dislocation suppression.

The (001) GaSb/GaAs interface and the structural defects in GaSb films were studied by TEM, both in cross-sectional and plan view. TEM specimens were prepared by mechanical polishing followed by  $\text{Ar}^+$  ion sputtering at liquid nitrogen temperature. Plan-view TEM specimens were thinned only from the substrate side: the GaSb film side was covered with crystal bond during mechanical thinning and was covered with glass plates during  $\text{Ar}^+$  ion sputtering. For preparation of cross-sectional TEM specimens, the wafer was first cleaved into small strips along the [110] and  $[1\bar{1}0]$  directions. The strips were then glued face-to-face and were polished using conventional techniques before ion-milling. TEM observation was carried out on a Philips EM 420 and a JEOL 4000 EX TEM operated at 120 and 400 keV, respectively. In order to achieve better statistics, measurements of dislocation densities were always carried out on plan-view specimens which were prepared near the epi layer top surfaces.

### Results and Discussion

The (001) GaSb/GaAs interface was studied using high-resolution TEM. Figure 1 shows the atomic resolution micrograph taken from the [110] cross section. The interface consists of a highly periodic array of perfect edge misfit dislocations along the [110] direction resulting in a semi-coherent interface. Burgers circuit drawn around each

individual dislocation shows that the Burgers vectors are of  $\mathbf{b} = \pm a/2[1\bar{1}0]$ , lying along the GaSb/GaAs interface. Each dislocation is associated with two extra {111} planes symmetrically located near the dislocation core (marked in Fig. 1). The measured misfit dislocation spacing ( $d = 57 \pm 2$  Å) is close to the predicted one and corresponds to a fully relaxed layer ( $d = \mathbf{b}/f = 55$  Å, where  $\mathbf{b}$  is the magnitude of misfit dislocation Burgers vector and  $f$  is the lattice mismatch). However, electron diffraction study reveals that there is about 0.6% compressive strain remaining in thin layers of GaSb. Direct observation of the interface shows that noticeable atomic displacements in both the substrate and epi layers are limited to within a few atomic layers from the interface. Another set of misfit dislocations is found to be along the  $[1\bar{1}0]$  direction which is also highly periodic. Similar misfit dislocation networks have been observed at the interfaces of (001)  $\text{In}_{0.11}\text{Ga}_{0.89}\text{Sb}/\text{GaAs}$  and (001) AlSb/GaSb.

Dislocations can nucleate under relatively low stress by the operation of dislocation sources. They can also nucleate spontaneously under high stress field. In small lattice mismatched heteroepitaxial systems where the misfit dislocations are mostly randomly spaced  $60^\circ$ , the misfit dislocations are generally thought to be formed either by elongating the existing threading dislocations or by nucleation of  $60^\circ$  dislocation half-loops near the epi layer surface which then glide on the {111} planes until they reach the interface plane to form misfit segments.<sup>14</sup> However, this mechanism presents difficulties when applied to the formation of the periodic network of  $90^\circ$  dislocations at the (001) GaSb/GaAs interface. Due to the sessile nature of the  $90^\circ$  dislocations on {111} planes, the formation of each  $90^\circ$  misfit dislocation may require two  $60^\circ$  dislocations to glide on particular {111} planes and to meet at the line of intersection of the two slip planes for interaction. Statistically this Lomer-Cottrell lock mechanism is not probable because the chance for two symmetric {111} slip planes to intersect exactly at the interface is small. Alternatively, dislocation climb relies on a nonequilibrium concentration of point defects; this scenario is not likely to occur under our growth conditions. Therefore, the nucleation of a highly periodic net of  $90^\circ$  misfit dislocations must be independent of the slip dislocations gliding on the {111} planes.

A separate experiment was carried out in order to investigate the initial stages of molecular beam epitaxy of GaSb on (001) GaAs substrates (see Ref. 10 for details). The misfit dislocation lines developed in individual islands line-up into a continuous line when the neighboring islands opalesce. However, we did not observe any apparent upward bending of these dislocation lines during the line-up process. As revealed by cross-sectional high-resolution transmission electron microscopy, the misfit dislocations in the interior of growing islands have a uniform spacing, but the spacing of the outermost one is often larger.<sup>10</sup> This suggests that misfit dislocations in the (001) GaSb/GaAs system nucleate spontaneously at the leading edges of advancing {111} planes of the GaSb islands where the stress fields have the highest values. After nucleation, they glide inward on the (001) interface plane to reach their

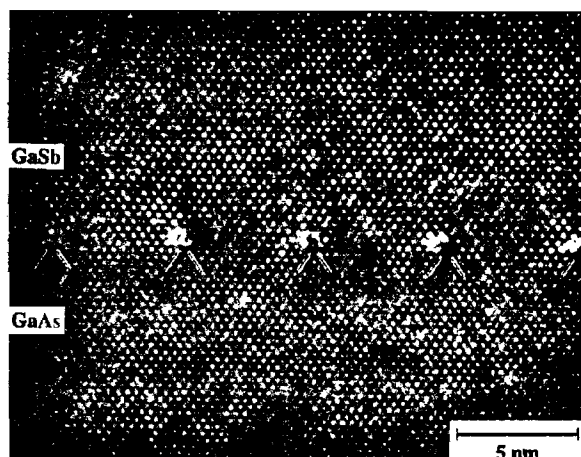


Fig. 1. Lattice image taken at the GaSb/GaAs interface along the [110] direction. A periodic array of  $90^\circ$  misfit dislocations with spacing of 5.7 nm are shown. Each dislocation is associated with two extra {111} planes as marked.

equilibrium positions. Since  $90^\circ$  misfit dislocations are twice as efficient as the  $60^\circ$  ones for strain relaxation (twice the Burgers vector components along the interface), only half the number of dislocation lines are required to accommodate a given misfit strain if  $90^\circ$  misfit dislocations are introduced instead of  $60^\circ$  ones. This is an energetically favorable state under suitable activation energy (provided by a suitable growth condition) and a sufficient driving force (provided by the large lattice constant mismatches).

Since  $90^\circ$  pure edge misfit dislocations are elastically stable, the defect density in the GaSb overlayer is relatively low considering the amount of lattice mismatch it has with the GaAs substrate. To a certain degree, the regular network of  $90^\circ$  misfit dislocations maximize the strain accommodation and minimize the amount of threading segments they introduce. However, inspection of a larger volume of the epi layer by conventional TEM shows that the GaSb film still contains many extended defects with their associated residual strains. The main defects are threading dislocations (with a number of stacking faults bounded by Shockley partials) which are uniformly distributed with an estimated density on the order of  $10^9$  to  $10^{10}/\text{cm}^2$ . The origin of these threading dislocations has been studied using samples with thin GaSb layers. It was found that every threading segment in the GaSb film is associated with the minority  $60^\circ$  misfit dislocations, which are generated either within the growing film or during coalescence of the growing islands.

The film thickness dependence of threading dislocation densities has been studied from a series of samples with different epi layer thicknesses grown under nominally the same condition. Their dislocation densities were determined near the epi layer top surface from plan-view specimens using conventional TEM techniques. Although cross-sectional TEM micrographs clearly show the distribution of threading dislocations at different film thicknesses, a quantitative measurement can be obtained more easily from plan-view specimens. Figure 2a and b show the plan-view micrographs taken from the GaSb films at thicknesses of 14 and 0.5  $\mu\text{m}$ , respectively. Under the identical diffraction condition ( $g = 220$ ) and imaging magnification, Fig. 2 shows an obvious reduction in threading density for thicker GaSb films ( $2 \times 10^7/\text{cm}^2$  at 14  $\mu\text{m}$ , compared with  $3 \times 10^9/\text{cm}^2$  at 0.5  $\mu\text{m}$ ). In Fig. 3, the measured threading densities are plotted against GaSb film thicknesses. As a general rule, the threading density decreases as the film thickness increases. Within the thickness range of  $0.5 \mu\text{m} \leq t \leq 14 \mu\text{m}$  which has been covered during this investigation, the dependence can be fitted as

$$\rho = 10^9/t^{5/3} \text{ (cm}^{-2}\text{)} \quad [1]$$

where,  $t$  is the epi layer thickness in micrometer.

The mechanism for dislocation reduction with increasing epi layer thickness is most likely related to the gliding of dislocations on the GaSb (111) planes under the action of residual compressive strain.<sup>11</sup> The majority of threading dislocations have  $a/2 \langle 110 \rangle$  type, Burgers vectors lying in (111) planes. By gliding, the dislocations can either form large misfit segments at the interface plane, annihilate each other during interaction of dislocations with opposite Burgers vectors, or form one new dislocation from two initial ones. All of these processes may reduce the number of dislocations which propagate through the epi layer. Since the threading dislocations are inclined with respect to each other, the probability for their mutual interaction increases as the film grows, resulting in significant threading dislocation density reduction at a large film thickness. In the region right above the interface, complicated dislocation interactions similar to those observed by Chu *et al.* in InP grown on GaAs were also observed.<sup>12</sup> However, it is interesting to compare our measurements with the results given by Sheldon and co-workers<sup>13</sup> for GaAs grown on (001) Si. The threading dislocation density in the (001) GaAs/Si system was about two times larger than that in

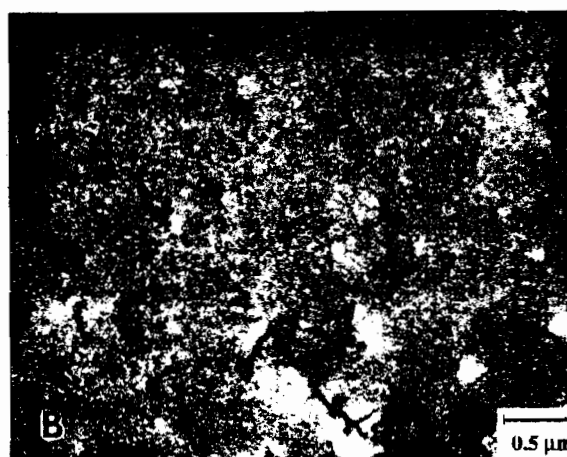


Fig. 2. Plan-view bright field micrographs ( $g = 220$ ) of GaSb epi layers taken at (a) 14 and (b) 0.5  $\mu\text{m}$  film thicknesses.

(001) GaSb/GaAs, even though the lattice mismatch is 8.2% in (001) GaSb/GaAs, compared with a 4.2% misfit in the (001) GaAs/Si system. Therefore, larger lattice mismatch does not necessarily result in higher density of threading dislocations. This can be attributed to the network of  $90^\circ$  misfit dislocations at the (001) GaSb/GaAs interface.

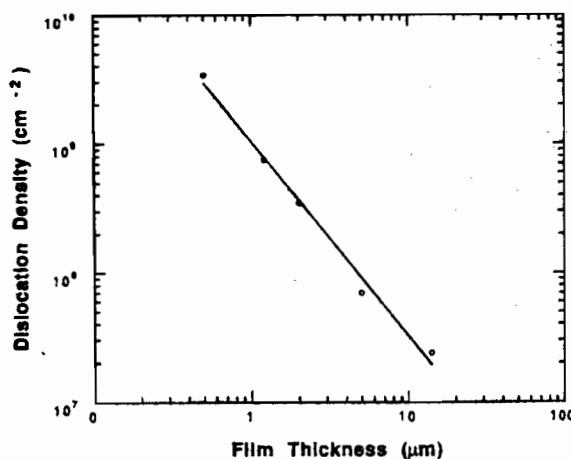


Fig. 3. Film thickness dependence of threading dislocation density in the GaSb thin films measured from plan-view TEM.



Fig. 4. C... effect of a...

Matthe... strained... location... at the int... (111) slip... either to... late one... the interf... epi layer... this study... GaSb thin... demonstr... field micr... buffer lay... has the... GaSb bu... and GaA... the bend... interface... dislocat... buffer/a... through... buffer la... that in t... ure qua... results... of  $\text{In}_{0.11}$ ... sities m... with di... Furth... deposit... ers. An... close to... was fo... tion re... section... with a... 1000 Å... bend b... which...

Table 1

Structu...

1.1  $\mu\text{m}$   
1.1  $\mu\text{m}$   
1.1  $\mu\text{m}$   
1.1  $\mu\text{m}$   
1.1  $\mu\text{m}$



Fig. 4. Cross-sectional bright field micrograph shows the blocking effect of an AlSb buffer to the threading dislocations.

Matthews and Blakeslee<sup>14</sup> were the first to propose that strained buffer layers can be used to reduce threading dislocation density in an epi layer. The stress field introduced at the interface may initiate the gliding of dislocations on {111} slip planes, causing the dislocation lines to bend either toward another threading line so that they annihilate one another or normal to the growth direction along the interface so that they do not propagate further into the epi layer. Different buffer layer schemes have been used in this study for threading dislocation density reduction in GaSb thin films. The effect of a single buffer layer can be demonstrated by Fig. 4. It shows a cross-sectional bright field micrograph taken from a sample with a 2000 Å AlSb buffer layer deposited underneath the GaSb layer. AlSb has the same cubic zinc blende structure as GaAs and GaSb but has 8.5 and 0.27% lattice mismatches with GaAs and GaSb, respectively. Figure 4 clearly shows the bending of threading dislocations near the AlSb/GaSb interface by the action of the strain field. The majority of dislocations are forced to propagate along the buffer/active layer interface rather than threading through the interface. The dislocation density within the buffer layer is at least one order of magnitude larger than that in the GaSb epi layer (although it is difficult to measure quantitatively from the cross-sectional image). Similar results were obtained by using a 1000 Å thick buffer layer of  $\text{In}_{0.11}\text{Ga}_{0.89}\text{Sb}$ . Table II summarizes the dislocation densities measured near the top surfaces of GaSb films grown with different buffer structures.

Further threading density reduction was achieved by deposition of structures containing multiple strained layers. An SLS of GaSb/AlSb with the thickness of each layer close to its critical value for misfit dislocation generation was found to be the most effective for threading dislocation reduction in the GaSb epi layer. Figure 5 is a cross-sectional bright field micrograph taken from the sample with a SLS composed of five periods of 1000 Å GaSb/1000 Å AlSb. The threading dislocation lines are forced to bend by the stress field exerted by the strained layer, which on one hand, increases the possibility for dislocation

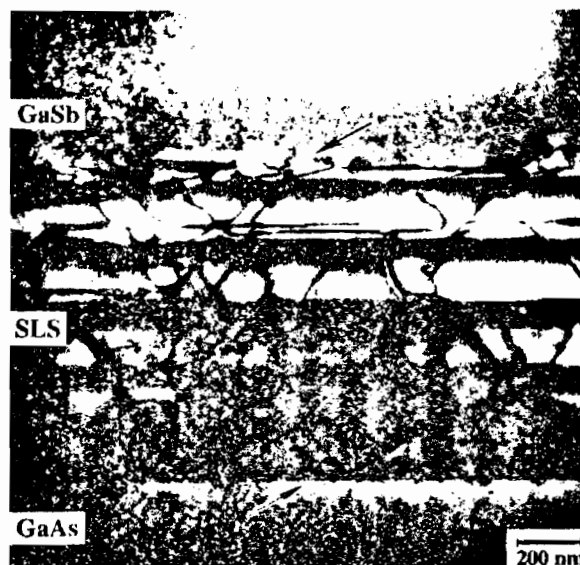


Fig. 5. Cross-sectional bright field micrograph shows the dislocation filtering of the GaSb/AlSb SLS. The majority of threading dislocations are bent by the SLS resulting in low defect density at the top GaSb layer.

interaction leading to dislocation annihilation and coalescence. On the other hand, some segments of threading dislocation lines become misfit dislocations at the interface. The threading dislocation lines were consecutively filtered out by the GaSb/AlSb layers. As a result, the threading dislocation density in the GaSb epi layer was reduced to the  $10^7/\text{cm}^2$  range using a structure containing nine interfaces. According to the formalism based on mechanical balance between the force exerted by the misfit strain and the tension in the dislocation line,<sup>14,15</sup> the critical thickness for GaSb grown on AlSb (with 0.27% lattice mismatch) is estimated to be about 2400 Å. However, Fig. 5 clearly shows that the formation of misfit dislocations started at film thickness of 1000 Å. Some threading segments are bent more easily for misfit strain relaxation. The bottom GaSb/GaAs interface (marked with an arrow) shows a regular array of closely spaced 90° misfit dislocations, since the critical thickness for a GaSb layer grown on GaAs is estimated to be less than 10 Å. The top GaSb/AlSb interface (marked with an arrow), however, consists of randomly spaced 60° misfit dislocations because of its small lattice match.

### Conclusion

One would expect that larger lattice constant mismatch often means a higher threading dislocation density in the epi layer. This is generally true for systems with relatively small lattice mismatches. In such systems, the misfit dislocations are mostly 60° which can easily glide on the {111} slip planes to form threading segments. Therefore, larger lattice mismatch means more misfit dislocations which often results in a higher threading density in the epi layer. However, in systems with very large lattice mismatches, such as GaSb grown on GaAs, the misfit dislocations are primarily 90° pure-edge, which are elastically stable. The defect density in the epi layer is thus relatively low despite their large lattice mismatches.

Threading dislocation density in GaSb epi layers depends inversely on the film thickness, due to interactions among dislocations which lead to mutual annihilation and coalescence. GaSb/AlSb SLS was found to be effective for threading dislocation suppression in the epi layer. The stress/strain field in the epi layer introduced by the SLS can initiate dislocation gliding on the {111} slip planes, causing the dislocation lines to bend either toward another threading line so that they annihilate one another

Table II. Threading dislocation densities in GaSb epi layers grown with different buffer schemes.

Structures	Threading dislocation density ( $\text{cm}^{-2}$ )
1.1 μm GaSb/1000 Å $\text{In}_{0.11}\text{Ga}_{0.89}\text{Sb}$ /GaAs	$9.5 \times 10^6$
1.1 μm GaSb/1000 Å AlSb/GaAs	$1.8 \times 10^6$
1.1 μm GaSb/2000 Å AlSb/GaAs	$1.2 \times 10^6$
1.1 μm GaSb/5000 Å AlSb/GaAs	$3.2 \times 10^6$
1.1 μm GaSb/5 × (1000 Å GaSb/1000 Å AlSb)/GaAs	$5.0 \times 10^7$



or normal to the growth direction along the interface so that they do not propagate further into the epi layer. The defect density in a 1  $\mu\text{m}$  thick GaSb film can be reduced to  $\sim 10^7/\text{cm}^2$  by the use of a SLS.

### Acknowledgments

W.Q. and M.S. acknowledge support under AFOSR Grant No. F29620.94.1.0392. R.K.'s work was performed at Wright Laboratory, Solid State Electronics Directorate, under Air Force Contract No. F33615-95-C1619.

Manuscript submitted June 20, 1996; revised manuscript received Jan. 2, 1997.

Carnegie Mellon University assisted in meeting the publication costs of this article.

### REFERENCES

1. S. F. Fang, K. Adomi, S. Iyer, H. Morkoc, H. Zabel, C. Choi, and N. Otsuka, *J. Appl. Phys.*, **68**, R31 (1990).
2. A. Hashimoto, N. Sugiyama, and M. Tamura, *Jpn. J. Appl. Phys.*, **30**, L447 (1991).
3. N. A. El-Masry, J. C. Tarn, and N. H. Karam, *J. Appl.*

- Phys.*, **64**, 3672 (1988).
4. J. W. Matthews, A. E. Blakeslee, and S. Mader, *Thin Solid Films*, **33**, 253 (1976).
5. K. Nozawa and Y. Horikoshi, *Jpn. J. Appl. Phys.*, **30**, L688 (1991).
6. G. H. Olsen, M. S. Abrahams, C. J. Buicocchi, and T. J. Zamerowski, *J. Appl. Phys.*, **46**, 1643 (1975).
7. T. Nishioka, Y. Itoh, M. Sugo, A. Yamamoto, and M. Yamaguchi, *Jpn. J. Appl. Phys.*, **27**, L2271 (1988).
8. C. Raisin, A. Rocher, G. Landa, R. Carles, and L. Lasabatere, *Appl. Surf. Sci.*, **50**, 434 (1991).
9. A. Rocher, *Solid State Phenom.*, **19&20**, 563 (1991).
10. W. Qian, M. Skowronski, R. Kaspi, and M. De Graef, *J. Appl. Phys.*, Submitted (1996).
11. A. Georgakilas and A. Christou, *J. Appl. Phys.*, **76**, 7336 (1994).
12. S. N. G. Chu, W. T. Tsang, T. H. Chiu, and A. T. Macrander, *ibid.*, **66**, 520 (1989).
13. P. Sheldon, K. M. Jones, M. M. Al-Jassim, and B. G. Yacobi, *ibid.*, **63**, 5609 (1988).
14. J. W. Matthews and A. E. Blakeslee, *J. Cryst. Growth*, **27**, 118 (1974).
15. J. W. Matthews and A. E. Blakeslee, *ibid.*, **29**, 273 (1975).

## Plasma Polymerization of Acetylene in a Box-Type Radio Frequency Gas Discharge Reactor under Plug Flow Condition

T. Uchida, G. K. Vinogradov,\* and S. Morita

Center for Cooperative Research in Advanced Science and Technology, Nagoya University, Nagoya 464-01, Japan

### ABSTRACT

Plasma polymerization of acetylene in a radio frequency discharge was studied under plug flow conditions in a box-type reactor with well-defined short range kinetic residence times beginning from the initial few milliseconds. Thin plasma polymerized films were deposited on semiconductor and metal surfaces and the process was monitored *in situ* by a quartz crystal microbalance and by optical emission spectroscopy. Pulsing the discharges provided a means of precise control of deposited thickness within a few angstroms. Secondary gas-phase products take part in the film formation beginning from about 30 to 40 ms of the kinetic residence time under the experimental condition. Post-discharge chemical reactions have a very small effect on the film thickness. The grafting, if any, of acetylene feed molecules on the plasma activated surface is negligibly small.

### Introduction

Plasma polymerization is a well-known deposition technique which forms thin cross linked organic films. During the deposition process the feed gas monomers undergo dissociation in the gas-phase plasma, with further transformations taking place after they are already incorporated in the deposited surface structure.

Certainly, plasma produces many kinds of reactive particles: electrons, ions, excited atoms and molecules, free radicals, and UV (ultraviolet) and VUV (vacuum UV) photons. Plasma electrons are principally responsible for the high rate nonselective excitation and decomposition of the feed gas molecules. This nonselective decomposition initiates multichannel chemical reaction mechanisms in the gas phase and on the surface, which greatly complicate the overall picture with hundreds of secondary molecular products interacting with the surface. Thus, the reactions of the initial feed gas molecules with the surface, which are the subject of numerous reports, are obscured and difficult to investigate.

We attempted to study and quantify some post-discharge deposition phenomena under well-defined conditions of short kinetic residence times using very light monomer acetylene as a model gas in order to exclude uncertainties originating from the kinetic nonideality of plasma polymerization reactors and the longtime adsorp-

tion-desorption equilibrium transitions typical for the vapors of heavy liquid monomers.

In order to simplify the model gas discharge object, one should strongly suppress the degree of gas-phase decomposition of the feed gas while the surface is still under the plasma activation.

Traditional approaches to decreasing the decomposition of initial molecular structures separates the active plasma zone from the deposition area. Therefore, the surface is separated from the plasma activation as well as the gas phase. Such conditions are very different from that of the active plasma zone. Hence, the experimental results obtained under such conditions can hardly be used to interpret plasma polymerization mechanisms.

There has long been a trend to describe the mechanisms of plasma polymerization on the basis of traditional free radical or ion chain reactions, accompanied by a subsequent plasma modification of the deposited linear polymer. However, as it was first suggested by Westwood,<sup>1</sup> the mechanism of plasma polymerization is a stepwise process of initiation and recombination (termination) reactions.

Many investigations concluded that the rate of plasma polymerization is not greatly dependent on the presence or absence of multiple unsaturated chemical bonds which are necessary for traditional chain polymerization reactions.<sup>2</sup> Gas-phase chain polymerization reactions are supposed to be negligible in gas discharges. Chain propagation reactions leading to the stepwise mass increase can be found among the known reactions of negative plasma ions with monomers. It was shown in the case of silane<sup>3</sup> and fluoro-

\* Electrochemical Society Active Member.

Current address: MC Electronics Co., 907-8, Shimomasa, Shiranecho, Nakakomagan, Yamanashi 400-02, Japan.

carbon  
thesis c  
lar par  
bution  
small,  
rate of  
to dep  
structu  
Surf  
Vacu  
and st  
is esse  
traditi  
cal ch  
found  
tiation  
1/600 f  
tron er  
active:  
mental  
cross s  
cross se  
range c  
Using a  
experim  
meriza  
about 3  
10 s. Th  
tion po  
tion in  
times o  
ferent f  
and Yas  
cal reac  
charge p  
dischar  
order of  
cle dec  
studyin  
chance  
reactio  
gas dis  
ed vap  
in a re  
for suc  
Here  
the sh  
ditions  
simult  
gas wi  
activa  
on" co  
suppre  
the se  
dence  
Plas  
dence  
RF ma  
Alcate  
tor. T  
(C<sub>2</sub>H<sub>2</sub>)  
The  
two t  
Teflon  
showe  
cross  
electr  
mm d  
and t  
low g  
such  
the g  
well-t  
analy